Geomicrobiology Journal

ISSN: 0149-0451 (Print) 1521-0529 (Online) Journal homepage: http://www.tandfonline.com/loi/ugmb20

Nitrogen Cycling of Active Bacteria within Oligotrophic Sediment of the Mid-Atlantic Ridge Flank

Brandi Kiel Reese, Laura A. Zinke, Morgan S. Sobol, Doug E. LaRowe, Beth N. Orcutt, Xinxu Zhang, Ulrike Jaekel, Fengping Wang, Thorsten Dittmar, Delphine Defforey, Benjamin Tully, Adina Paytan, Jason B. Sylvan, Jan P. Amend, Katrina J. Edwards & Peter Girguis

To cite this article: Brandi Kiel Reese, Laura A. Zinke, Morgan S. Sobol, Doug E. LaRowe, Beth N. Orcutt, Xinxu Zhang, Ulrike Jaekel, Fengping Wang, Thorsten Dittmar, Delphine Defforey, Benjamin Tully, Adina Paytan, Jason B. Sylvan, Jan P. Amend, Katrina J. Edwards & Peter Girguis (2018): Nitrogen Cycling of Active Bacteria within Oligotrophic Sediment of the Mid-Atlantic Ridge Flank, Geomicrobiology Journal, DOI: 10.1080/01490451.2017.1392649

To link to this article: https://doi.org/10.1080/01490451.2017.1392649

Published online: 15 Feb 2018.

GEOMICROBIOLOGY JOURNAL
https://doi.org/10.1080/01490451.2017.1392649

Taylor & Francis
Taylor & Francis Group

Nitrogen Cycling of Active Bacteria within Oligotrophic Sediment of the Mid-Atlantic Ridge Flank

Brandi Kiel Reese[a], Laura A. Zinke[a,b], Morgan S. Sobol[a], Doug E. LaRowe[b], Beth N. Orcutt[c], Xinxu Zhang[d], Ulrike Jaekel[e], Fengping Wang[d], Thorsten Dittmar[f], Delphine Defforey[g], Benjamin Tully[b], Adina Paytan[g], Jason B. Sylvan[h], Jan P. Amend[b], Katrina J. Edwards[#], and Peter Girguis[d]

[a]Department of Life Sciences, Texas A&M University-Corpus Christi, Corpus Christi, TX, USA; [b]Department of Biological Sciences, University of Southern California, Los Angeles, CA, USA; [c]Bigelow Laboratory for Ocean Sciences, East Boothbay, ME, USA; [d]School of Life Sciences and Biotechnology, Shanghai Jiao Tong University, Shanghai, China; [e]Department of Organismic and Evolutionary Biology, Harvard University, Boston, MA, USA; [f]Institute for Chemistry and Biology of the Marine Environment, University of Oldenburg, Max Planck Institute, Oldenburg, Germany; [g]Institute of Marine Sciences, University of Santa Cruz, Santa Cruz, CA, USA; [h]Department of Oceanography, Texas A&M University, College Station, TX, USA

ABSTRACT

Microbial ecology within oligotrophic marine sediment is poorly understood, yet is critical for understanding geochemical cycles. Here, 16S rRNA sequences from RNA and DNA inform the structure of active and total microbial communities in oligotrophic sediment on the western flank of the Mid-Atlantic Ridge. Sequences identified as Bacillariophyta chloroplast were detected within DNA, but undetectable within RNA, suggesting preservation in 5.6-million-year-old sediment. Statistical analysis revealed that RNA-based microbial populations correlated significantly with nitrogen concentrations, whereas DNA-based populations did not correspond to measured geochemical analytes. Bioenergetic calculations determined which metabolisms could yield energy *in situ*, and found that denitrification, nitrification, and nitrogen fixation were all favorable. A metagenome was produced from one sample, and included genes mediating nitrogen redox processes. Nitrogen respiration by active bacteria is an important metabolic strategy in North Pond sediments, and could be widespread in the oligotrophic sedimentary biosphere.

ARTICLE HISTORY
Received 28 February 2017
Accepted 11 October 2017

KEYWORDS
Biogeochemistry; deep biosphere; IODP; N cycle; oligotrophic sediment; RNA

Introduction

A large portion of the Earth's total biomass is sequestered in marine sediment as microbial cells. An estimated 4.1 petagrams of C, or 0.6% of total living biomass, reside in the deep sediment subsurface as microorganisms (Kallmeyer et al. 2012). This important biosphere is responsible for the remineralization of nutrients and carbon essential to sustain life and fuel global biogeochemical cycles. It is uncertain however, what fraction of the marine subsurface microbial biomass is metabolically active, inactive, or dead, and what is the structure and diversity of microbial communities in these environments. Recent work has shown that microbes are active in oligotrophic sediment underlying the South Pacific Gyre (D'Hondt et al. 2015; Meyer et al. 2016), but recovering biomass for determining microbial community structure and the fraction of active versus inactive cells has proven challenging except in high organic carbon containing sediment samples (Durbin and Teske 2011).

Dormancy or inactivity is a common mechanism for survival in unfavorable conditions such as energy and nutrient limitation, extreme temperature, or pressure. A combination of all of these conditions is characteristic of deep subsurface sediments. Although these environmental conditions are widespread in the deep biosphere, there is still a lack of understanding about how the presence of inactive subsurface microbes skews the interpretation of microbial community functional and structural diversity. Overall, the fraction of the microbial community that is viable but metabolically inactive can be variable, and sometimes quite large, ranging from 20% to 80% (Jones and Lennon 2010). The abundance of endospores or inactive cells might be equal to actively growing microorganisms in the deep subsurface (Lomstein et al. 2012). DNA may be detected in cells that are dormant or living, and extracellular DNA is more likely to be preserved in marine sediments than RNA due to the preferential binding of DNA to organic molecules and the shorter half-life of most RNA (Corinaldesi et al. 2011).

Molecular tools may be used to assess the structure of microbial communities by simultaneously characterizing the active community through ribosomal RNA-based analysis (sequencing of rRNA molecules) and the total community through ribosomal RNA gene-based analysis (sequencing of DNA). The fraction of the community that is not detected in the RNA sequences, but observed in the DNA sequences, can be attributed to inactive organisms or a result of 16S rRNA gene transcript abundance below the detection limit (Mills et al. 2005), though with some caveats (Blazewicz et al. 2013). A majority of previous studies have relied almost exclusively on

CONTACT Brandi Kiel Reese brandi.reese@tamucc.edu Department of Life Sciences, Texas A&M University-Corpus Christi, Corpus Christi, TX, USA.
Color versions of one or more of the figures in the article can be found online at www.tandfonline.com/ugmb.
[#]Deceased.

DNA analysis (and therefore putative function) of the microbial community to infer the dominant biogeochemical cycles of the environment (Biddle et al. 2008; Stein et al. 2014). However, if DNA is derived from inactive microbes or extracellular DNA, the conclusions of these studies may be misleading (Torti et al. 2015). Documenting the fraction of the microbial population that is metabolically active, and how this relates to sediment geochemical parameters, is important to understand which microbial groups are responsible for carbon remineralization under varying conditions.

Sediment collected from the western flank of the Mid-Atlantic Ridge during Integrated Ocean Drilling Program (IODP) Expedition 336 (Expedition 336 Scientists 2012) provided an opportunity to evaluate the active versus total microbial communities in oligotrophic, oxic marine sediment environments, and to assess how these two communities might influence sediment biogeochemistry. IODP Expedition 336 cored sediment within "North Pond"—a sediment-filled depression overlying young basaltic basement where dissolved chemical profiles revealed oxic water-sediment and sediment-basement interfaces bracketing suboxic to anoxic interior sections (Orcutt et al. 2013). The opposite was observed in dissolved nitrate; nitrate was highest in the center of the sediment columns, and lower at the water-sediment and sediment-basement interfaces (Expedition 336 Scientists 2012; Wankel et al. 2015). Recent studies determined that the porewater nitrate isotopic composition and profiles reflects active redox cycling of nitrogen, including the co-location of oxidative and reductive transformations at North Pond (Wankel et al. 2015).

Here, we describe the structure of active and total (i.e., living, inactive, dead) microbial communities in sediment samples from North Pond. A method was used to simultaneously extract both RNA and DNA from oligotrophic sediment for sequencing of 16S rRNA gene transcripts (active, RNA-derived) and 16S rRNA genes (total, DNA-derived). Simultaneous extraction of DNA and RNA permits the analysis of the total and the active populations, respectively, from a single sample, thus avoiding biases associated with heterogeneity common in sediment communities. We hypothesized that the identity of the active community determined by 16S rRNA gene transcripts more closely matches community structure expectations based on dominant biogeochemical reactions (e.g., nitrification, denitrification), whereas the total community reflects inactive or dead cells that will not be correlated with sediment geochemical parameters.

Methods

Sample collection

Samples were collected in September-November 2011 during IODP Expedition 336 to North Pond, an isolated sediment pond located approximately 140 km west of the Mid-Atlantic ridge axis (Figure 1). Water depth on site ranged from 4425 to 4494 m. Two holes, U1382B (22°45.353′N, 46°04.891′W) and U1383D (22°48.133′N, 46°03.156′W), were drilled using Advanced Piston Coring (APC) to a terminal depth of 90 and 43.3 meters below seafloor (mbsf), respectively (Expedition 336 Scientists, 2012). Samples were collected from the top, middle, and bottom of each hole, including core sections U1382B-1H4 (4.7 mbsf), U1382B-6H3 (46.7 mbsf), U1382B-9H4 (77.1 mbsf), U1383D-2H3 (8.9 mbsf), U1383D-4H2 (26.0 mbsf), and U1383D-5H4 (38.6 mbsf; summarized in Table 1). From each section, a 10-cm-long whole round core was cut, capped on both ends with ethanol-cleaned caps, and stored at −80°C until transported on dry ice.

Potential contamination from drilling was assessed on board by inspecting the integrity of the core liner and analyzing for the presence of fluorescent microspheres derived from drilling mud on adjacent samples to those used for analysis (Expedition 336 Scientists 2012). All of the deeper cores selected for analysis in this study had no shipboard evidence for microsphere contamination of the interior, while the exteriors did have microsphere contamination; the two shallowest samples, which were very sandy, did show some evidence of microsphere intrusion to the interior of the core (Expedition 336 Scientists 2012). Samples were reanalyzed in a shore-based lab for the presence of microspheres and none were noted. Additionally, aliquots of the drilling mud were also collected and preserved for nucleic acid extraction as a control to evaluate contamination.

Pore water and solid phase geochemical data (e.g., anions, cations, total organic carbon (TOC), and total nitrogen (TN)) were collected both shipboard and onshore; those methods and results are reported elsewhere (Expedition 336 Scientists 2012). Oxygen was measured shipboard using microsensors (Orcutt et al. 2013). All geochemical data provided by collaborators for the purpose of statistical analysis are reproduced here with permission.

Cell enumeration

As described elsewhere (Expedition 336 Scientists 2012), sediment samples were fixed while on board in a formaldehyde solution for later analysis by collaborators at Shanghai Jiao Tong University following a modified protocol for low-biomass samples (Kallmeyer et al. 2008; Lever et al. 2010). Cells were extracted from sediment in triplicate. Carbonate was removed from 100 μl of the preserved sediment slurry with 500 μl of an acetate buffer for 2 h, followed by centrifugation at 3000 × g for 5 min. The supernatant was removed for enumeration and the remaining pellet was resuspended with 500 μl of 3.5% NaCl, 50 μl of detergent mix (100 mM disodium EDTA dehydrate, 100 mM sodium pyrophosphate decahydrate, 1% vol/vol Tween 80, and NaCl to approximate seawater salinity), and 50 μl of methanol. After vortexing overnight at room temperature, 500 μl of 50% (wt/vol) Nycodenz was added below the slurry and centrifuged at 1500 × g for 10 min. The supernatant was removed and combined with the supernatant in the previous step. The remaining pellet was resuspended by sonication in an ice bath three times for 10 s intervals each. Addition of Nycodenz followed by centrifugation was repeated as above and the supernatant was transferred to the same tube. All layers were combined and were used for enumeration. The combined supernatant was filtered through 0.2-μm-mesh GTBP membrane (Millipore) filter and stained with SYBR Green I solution (1:40 vol/vol SYBR Green I in TE buffer) for 20 min. Cells were counted at 1000× magnification using epifluorescence

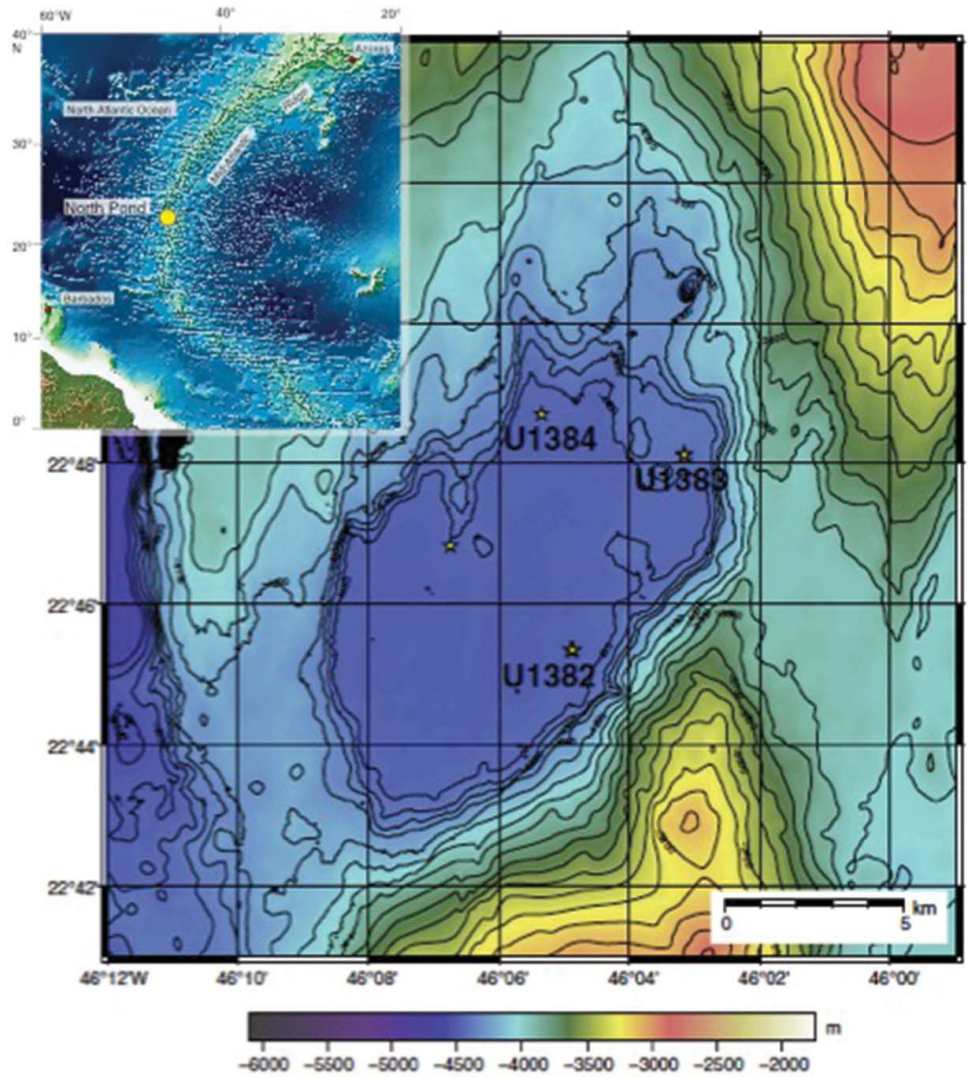

Figure 1. Map depicting the sediment sample locations from IODP Expedition 336 to the western flank of the Mid-Atlantic Ridge, as modified from (Orcutt et al. 2013). Inset shows the location of the site on the Mid-Atlantic Ridge, overlain on detailed map of the sediment pond at the North Pond site, with contour lines at 100m intervals and water depth scale shown in meters.

microscope (Nikon ECLIPSE 90i; Japan) with a blue filter (FITC). An average of 270 fields were counted for each membrane and images were analyzed by NIS-Elements AR software (Nikon, Japan).

Nucleic acid extraction

Nucleic acids were extracted from six frozen sediment cores using a method to simultaneously extract both DNA and RNA from low biomass environments, reducing biases that can arise from separate extractions (Reese et al. 2013). Three samples each were chosen from Hole U1382B and U1383D cores, representing the upper oxic, middle suboxic to anoxic, and lower oxic sections of the sediment column at each location (Table 1). To reduce potential contamination from drilling fluid that may have penetrated the ends of the core, sediment sections from the middle of the whole core length were selected. Subsamples for extraction were removed from the frozen interior of the core cylinder using a sterile spatula. Facemasks and hair caps were worn throughout, and extractions took place in a laminar flow hood to reduce human and aerosol contamination.

The following protocol steps are a modification of a previously published method (Reese et al. 2013). All chemicals were molecular biology grade (MBG), solutions were treated with diethylpyrocarbonate (DEPC) and autoclaved, and glassware was baked at 500°C before use. Approximately 0.5 g of frozen sediment from the center of whole round cores was placed into 2 ml tubes. Each sample received 150 μl of extraction buffer [200 μl of 500 mM EDTA (EMD Chemicals, Gibbstown, NJ, USA; pH 8.0), 230 μl of 40% glucose (Calbiochem; La Jolla, CA, USA), and 250 μl of 1 M Tris-HCl (MP Biomedicals; Solon, OH, USA; pH 8.0) raised to a final volume of 10 ml with DEPC-treated water], for a final concentration 0.92% glucose, 10 mM EDTA, and 25 mM Tris-HCl. Buffered samples were subjected to five rounds of vortexing for 1 min, flash freezing in liquid nitrogen, and thawing in a 55°C water bath for 1 min. After five cycles, 50 μl of 500 mM EDTA (pH 8.0) and 250 μl of extraction buffer amended with 4 mg/ml lysozyme (Rockland, Inc; Gilbertsville, PA, USA) and 4 mg/mL Proteinase K (Sigma Aldrich; Saint Louis, MO, USA) were added to each sample. After mixing with a vortex for approximately 1 min, samples were incubated at 30°C for 10 min while shaking at

Table 1. Summary of sample depth, number of quality-controlled 16S rRNA gene sequences per sample, and 16S rRNA gene OTU abundance for RNA and DNA fractions, and microsphere detection from North Pond IODP Expedition 336 sediment samples.

Location	Depth (mbsf)	Sequences	OTUs*	Evenness	Shannon	Microsphere**
1382B 1H4 DNA	4.7	7831	149	0.74	3.70	+
1382B 6H3 DNA	46.7	8207	192	0.78	4.08	–
1382B 9H4 DNA	77.1	10479	189	0.78	4.06	–
1383D 2H3 DNA	8.9	8124	136	0.78	3.82	+
1383D 4H2 DNA	26.0	6634	121	0.76	3.64	–
1383D 5H4 DNA	38.6	3614	93	0.78	3.55	–
1382B 1H4 RNA	4.7	3594	96	0.75	3.44	+
1382B 6H3 RNA	46.7	922	38	0.48	1.75	–
1382B 9H4 RNA	77.1	2457	66	0.69	2.88	–
1383D 2H3 RNA	8.9	5764	102	0.61	2.81	+
1383D 4H2 RNA	26.0	8413	114	0.55	2.63	–
1383D 5H4 RNA	38.6	8601	141	0.37	1.83	–

*Number of operational taxonomic units (OTU) determined at 95% similarity on normalized sequence abundance.

**Microspheres analyzed during shipboard analysis detected on the interior of the core indicated qualitatively: – = no microspheres detected, + = <1 microsphere per field of view (FOV), ++ = 1–5 microspheres/FOV, +++ = 5–10 microspheres/FOV (Expedition 336 Scientists, 2012) mbsf = meters below seafloor.

200 rpm. A volume of 50 μl of 10% solution of sodium dodecyl sulfate (SDS) (Sigma Aldrich; Saint Louis, MO, USA) was added to each sample. This was homogenized gently and half (~400 μl) of the sediment-SDS slurry was transferred to a clean 2 ml tube using a sterile wide-bore pipette tip. A solution of unbuffered phenol (pH 6.4):chloroform:isoamyl alcohol (25:24:1) was added to the remaining sediment-SDS mixtures at 800 μl. The acidic pH favors RNA extraction, and the final extract was used for reverse transcription and cDNA amplification. As a modification to the previously published method, 800 μl of 25:24:1 Tris-HCl buffered phenol (pH 8.0):chloroform:isoamyl alcohol was added to the transferred sediment in order to extract DNA from half the sample. The circumneutral pH favors DNA extraction, and the final extract was used for DNA amplification.

All samples were vortexed for 1 min and centrifuged at room temperature for 3 min at 15,000 rpm. The top aqueous phase was transferred to 2 ml tubes with 800 μl of fresh phenol:chloroform:isoamyl alcohol. The pH of the phenol solution for samples was the same as previously used: acidic for RNA extraction and basic for DNA extraction. All samples were vortexed for 1 min and centrifuged at room temperature at 15,000 rpm for 3 min. The aqueous phase was transferred to sterile 1.5 ml centrifuge tubes. To each sample, 50 μl of 3 M sodium acetate was added (J. T. Baker; Phillipsburg, NJ, USA) and at least 1 ml 200 proof MBG ethanol was added. Samples were centrifuged at 15,000 rpm for 15 min at 4°C. Supernatant was removed and pellets dried near open flame for approximately 10 min, or until no visible traces of ethanol remained. Samples extracted for RNA were resuspended in 50 μl of 0.01 M sodium citrate (pH 6.4), and residual DNA was removed using Turbo DNA Free (Ambion Inc.; Austin, TX, USA) following manufacturer protocol. Samples extracted for DNA were resuspended in basic (pH 8) water.

To increase yield, 10 tubes of sediment, or 5 g of sediment total, were extracted simultaneously and the resulting pellets were serially pooled. Extraction controls containing no template and sterile water were carried out throughout the extraction and sequencing process. Resulting DNA and RNA extracts were quantified using a Qubit fluorometer (Thermo Scientific, Waltham, MA, USA) and quality was checked on a NanoDrop 1000 Spectrophotometer (Thermo Scientific, Waltham, MA, USA) prior to shipment to the sequencing facility (Research and Testing Laboratory; Lubbock, TX, USA).

One sample (U1382B-7H5; 59.7 mbsf) was extracted for the purposes of metagenomic analysis. Other samples were attempted; however, this sample had the most successful recovery. U1382B-7H5 was located within the nearly anoxic region of the sediment column. Twenty replicate tubes containing 0.5 g of sediment were extracted for total DNA using the phenol-chloroform method described above. The extraction was checked for DNA quantity and quality using the methods described for 16S rRNA gene analysis and was sent for sequencing at the Marine Biological Laboratory (Woods Hole, MA, USA).

The extraction of DNA and RNA was also tested using commercially available kits in addition to the method described herein; however, the yield from the kits was an order of magnitude less than that of this method (data not shown). This is consistent with other studies that have compared phenol-based methods and commercial kits (Lever et al. 2015; Lloyd et al. 2010). In oligotrophic sediments with low humic acid concentrations such as North Pond, clean-up procedures employed by commercial kits are often unnecessary, as they also tend to remove nucleic acids, and thus decrease the overall yield (Lever et al. 2015).

Reverse transcription of RNA

DNase-treated RNA extracts were reverse-transcribed to complementary DNA (cDNA) using moloney murine leukemia virus (MMLV) reverse transcriptase (Promega; Madison, WI, USA). The Bacteria 16S rRNA gene primer 518R was used (5′-CGT ATT ACC GCG GCT GCT GG-3′) (Nogales et al. 1999) to target the 16S rRNA for cDNA generation. RNA was incubated for 5 min at 70°C, followed by the addition of the reverse transcription (RT) reaction mixture, and a subsequent incubation for 60 min at 30°C. The RT reaction mixture contained 1X M-MLV buffer (50 mM Tris-HCl, 3 mM $MgCl_2$, 75 mM KCl, and 10 mM DTT; Promega, USA), 10 mM deoxynucleotide triphosphate solution mix (New England Biolabs, USA), 1 U of M-MLV enzyme (Promega, USA), and molecular grade water. This resulted in cDNA, which was later amplified using PCR.

Amplification and sequencing

DNA extracts and reverse-transcribed cDNA were amplified using PCR with the *Bacteria* 16S rRNA gene forward primer

27F (Giovannoni et al. 1991) and reverse primer 518R, spanning the V1–V3 hypervariable regions. Sequencing of archaeal 16S rRNA genes was not attempted, as this was within the purview of a complimentary sample request for Expedition 336. The PCR reaction mixture was 1X buffer [10 mM KCl, 10 mM $(NH_4)_2$ SO_4, 20 mM Tris-HCl, 2 mM $MgSO_4$, 0.1% Triton X-100; New England Biolabs, USA], 10 mM deoxynucleotide triphosphate solution (New England Biolabs, USA), 1 U of *Taq* DNA Polymerase (New England Biolabs, USA), and molecular grade water. Reaction conditions were 95°C for 5 min, 35 cycles of 95°C for 30 sec, 50°C for 30 sec, and 72°C for 30 sec, and 72°C for 10 min. Reaction products were visualized on 0.7% agarose, ethidium bromide-stained gels, and illuminated using UV light. The extraction blanks were PCR amplified at 55 cycles to identify potential contamination and were sequenced despite lack of visible amplification. No-template controls to ensure contamination-free reactions were performed alongside both RT and PCR reactions, and showed no amplification. Picogreen (ThermoFisher Scientific, Grand Island NY) was used to quantify amplification products.

DNA and cDNA amplicons were checked for quality and sequenced using a 454 FLX Sequencer (454 Life Science, Branford, CT, USA) at the Research and Testing Laboratory (Lubbock, TX, USA) following standard protocols. Sequences were denoised and screened at Research and Testing Laboratory for minimum read length of 250 base pairs and minimum quality scores of 25. The 16S rRNA gene nucleotide sequences from DNA and RNA (via cDNA) have been deposited in the National Center for Biotechnology Information (NCBI) database under BioProject number PRJNA308331.

Metagenome library construction and sequencing was performed at the Marine Biological Laboratory Keck facility through the Deep Carbon Observatory's Census of Deep Life program (Vineis et al. 2016). Picogreen (ThermoFisher Scientific, Grand Island NY) was used to quantify genomic DNA samples. 15 ng DNA was sheared using a Covaris S220 (Covaris, Woburn MA) and libraries are constructed with the Ovation Ultralow Library protocol (Nugen, San Carlos CA) and amplified for 18 cycles. The amplified product was visualized on a Bioanalyzer DNA 1000 chip (Agilent Technologies, Santa Clara CA). Libraries were size selected using a PippinPrep 1.5% cassette (Sage Science, Beverly MA) to an average insert size of 170 bp (280 bp including adapters). The amount of genetic material was quantified by qPCR (Kapa Biosystems, Wilmington, MA), and sequenced on the Illumina HiSeq1000 (Illumina, San Diego, CA, USA) in a paired-end sequencing run (2 × 150) using dedicated read indexing. The sample datasets were demultiplexed with CASAVA 1.8.2. The metagenomic sequences may be accessed through the Marine Biological Lab Visualization and Analysis of Microbial Population Structures database (Huse et al. 2014).

Quality control and bioinformatic analysis of sequences

To account for possible sources of contamination, sequences from the samples in this study were compared to sequences generated from the negative extraction controls (V1–V3) and from the drilling mud used during the expedition (extracted using different methods and amplifying the V6 region; generated at the Marine Biological Laboratory, BioProject PRJNA280201) (Meyer et al. 2016).. The sequences obtained from the extraction negative control and drilling mud extraction were clustered in *Qiime* to the *Greengenes* (updated October 2, 2011) reference database (DeSantis, Hugenholtz et al. 2006). *Sourcetracker* was then used to identify any overlapping operational taxonomic units (OTUs) called as the same species at the 97% or greater sequence similarity level, which were removed from further analysis (Knights et al. 2011), as a conservative measure of contamination assessment (Inagaki et al. 2015). The resulting sequences were reanalyzed using a combination of the programs *Qiime* (Caporaso et al. 2010) and *mothur* (Schloss et al. 2009). Chimeric sequences were removed using *Chimera Slayer* within *mothur* (Haas et al. 2011). Using the pick_open_reference_otus.py command in *Qiime*, sequences were aligned and clustered against Greengenes (October 2011) into OTUs at ≥95% sequence similarity threshold and reads that did not align to the reference were *de novo* clustered at ≥97% sequence similarity

Community beta diversity analyses of the OTUs were performed in *mothur* using Bray-Curtis similarity index within *mothur*, which normalized sequence abundance to the sample with the least number of sequences. Alpha diversity indices including evenness and Shannon were calculated from the 95% similarity OTUs within *Qiime* (Table 1). Sequences were assigned a taxonomic classification at a 97% identity threshold (approximately equivalent to a genus level classification) at a confidence interval of >80% using the Ribosomal Database Project (RDP) classifier version 2.10.1 (Wang, Garrity et al. 2007). Representative sequences corresponding to OTUs assigned to *Cyanobacteria* were checked against the National Center for Biotechnology Information (NCBI) nucleotide database using the Basic Local Alignment Search Tool (BLASTn). NET algorithm (accessed March 2013) (Dowd et al. 2005). The taxonomic classifications of the drilling mud sequences identified in this study is provided as a Supplemental Figure 1.

Metagenomic reads were quality filtered and adapters were removed using Cutadapt (v1.7.1) (Martin 2011) with a minimum e-value of 0.08. Sequences were trimmed using Trimmomatic (v 0.33) (Bolger et al. 2014) with a 10bp sliding window with quality score cutoff of 28 and a minimum length of 75. Reads passing quality control and filtering were assembled using IDBA-UD (v1.1.1) (Peng et al. 2012). Gene coding sequences were predicted using Prodigal (Hyatt et al. 2010), and resulting sequences were assigned KEGG Ontology (KO) identifiers using GhostKOALA (Kanehisa et al. 2016). Putative coding sequences assigned KOs involved in nitrogen cycling were taxonomically classified using NCBI-RefSeq (BLASTP search; e-value cutoff 1×10^{-5}) and the MEGAN (V4) Last Common Ancestor algorithm (Huson et al. 2007).

Quantitative PCR

The bacterial 16S rRNA gene transcripts for Hole U1383B sediment samples were quantified using quantitative PCR (qPCR). Standards for the 16S rRNA gene were generated from whole extract of a mixed bacterial community using the 331F (5′-TCC TAC GGG AGG CAG CAG T-3′) and 797R (5′-GGA CTA CCA GGG TAT CTA ATC CTG TT-3′) primers in a PCR reaction (Nadkarni et al. 2002). Amplicons were visualized on agarose gels, the corresponding band was excised, and

amplicons were purified according to manufacturer instructions using the QIAquick PCR purification kit (Qiagen, Valencia, CA, USA). Standard concentrations were measured in triplicate using a NanoDrop 1000 Spectrophotometer (Thermo Scientific, Waltham, MA, USA). Copy number was calculated assuming a molecular mass of 660 Da for a base pair of DNA and using the following formula: Copy Number = [6.023 × 10^{23} (bp/mol/bp) × concentration of standard (ng/l)] / [PCR Product Size (bp gene copy^{-1}) × 10^{9} (ng/g) × 660 (g/mol/bp)] (Jin and Mattes 2010). Concentrations of standards ranged from a detection limit of 10^{2} to 10^{7} copies per reaction. Amplicons from cDNA generation and standards were analyzed in triplicate using the 331F and 518R primers and SYBR green assay on the StepOnePlus Real-Time PCR System (Applied Biosystems, Foster City, CA, USA). Reaction conditions followed SYBR-Green manufacturer instructions, with optimized primer concentration conditions. Results were analyzed using the StepOne Software 2.0 package (Applied Biosystems, Foster City, CA, USA).

Statistical analyses

Pearson correlation coefficients were calculated between biological and geochemical factors. The influence of nitrogen, phosphorous, sulfur, oxygen, dissolved organic carbon (DOC), and total organic carbon (TOC) on the observed bacterial OTU distribution was statistically analyzed through a Multi-Response Permutation Procedure (MRPP). Principal Component Analyses (PCA) were performed in PC-ORD software (McCune and Mefford 1999). Singular Value Decomposition (SVD) and Student's *t*-tests were performed in Microsoft Excel® using PopTools. SVD is a multivariate statistical method used to find patterns in data in order to understand the correlation between both the active and total community with the respective geochemical data. Geochemical and phylogenetic data was first transformed using either chi-square or arcsine statistical tests, where appropriate, and normalized prior to SVD and PCA analyses (Box and Cox 1964; Conner and Hartl 2004). A Monte Carlo simulation with 10,000 iterations was performed on statistical analyses to verify significance. Kaiser's Rule was implemented in order to decrease the original 23 geochemical constituents incorporated into the PCA to just six constituents for further analysis (Figure 7b). In brief, the number of variables equal to the number of eigenvalues may be selected based on the regression significance when correlation based matrix is used in PCA (Jolliffe 2002).

Bioenergetics

Values of the Gibbs energy of reaction, ΔG_r, are calculated using

$$\Delta G_r = -RT \ln \frac{K_r}{Q_r} \quad (1)$$

where K_r and Q_r refer to the equilibrium constant and reaction quotient of the reaction, respectively, R represents the gas constant in units of J/K/mol, and T denotes temperature in Kelvin. Values of K_r were calculated using the revised-HKF equations of state (Helgeson, Kirkham et al. 1981, Tanger and Helgeson 1988, Shock, Oelkers et al. 1992), the SUPCRT92 software package (Shock, Oelkers et al. 1992), and thermodynamic data taken from a number of sources (Schulte et al. 2001; Shock and Helgeson 1988; 1990; Shock et al. 1989). Values of Q_r were calculated using

$$Q_r = \prod_i a_i^{\upsilon_i} \quad (2)$$

where a_i stands for the activity of the ith species and ν_i corresponds to the stoichiometric coefficient of the ith species in the reaction of interest. Values of a_i are related to the concentration of the ith species, C_i, through

$$a_i = \gamma_i \left(\frac{C_i}{C_i^{\theta}} \right) \quad (3)$$

where γ_i stands for the activity coefficient of the ith species and C_i^{θ} refers to the concentration of the ith species under standard state conditions, which is taken to be equal to 1 molal referenced to infinite dilution. Values of γ_i were in turn computed as a function of temperature and ionic strength using an extended version of the Debye–Hückel equation (Helgeson 1969). Geochemical data provided through shore-based and shipboard analyses were used in conjunction with the Spec8 speciation program in Geochemist Workbench (Champaign, IL, USA) to determine values of C_i.

Concentration data for the inorganic reactions shown in Table 2 came from published data (Expedition 336 Scientists 2012; Orcutt et al. 2013). Ammonium was reported as below the detection limit (1.5 μM in samples from Hole U1382B and 6 μM in samples from Hole U1383D) in all samples; therefore, we assumed a value of 1.0 μM for the calculations. Oxygen concentrations were above detection limit except one sample (U1382B-2H2), which we assumed a value of 1.0 μM for the calculations. The average stoichiometry of the several thousand molecular formulae identified in DOM was $C_{27}H_{28}O_7$ (LaRowe and Van Cappellen). For the heterotrophic reactions, $C_{27}H_{28}O_7$ is used as a proxy for the complex suite of organic compounds that are found in marine sediments. In addition, the average nominal oxidation state of carbon (NOSC) in $C_{27}H_{28}O_7$ is −0.52 and the average NOSC of the DOM for the six samples locations is −0.51. Given that the amount of energy available from organic matter is strongly correlated with its NOSC

Table 2. Free energy available per volume of sediment and per mole of electrons from the indicated reactions based on *in situ* parameters, taking the limiting reactant into account.

	Denitrification		Nitrification		N_2 fixation	
Location	J/cm^3	kJ/(mol e-)	J/cm^3	kJ/(mol e-)	J/cm^3	kJ/(mol e-)
U1382B-1H4	17.44	−98.77	0.33*	−65.48*	1.09*	−4.36*
U1382B-6H3	17.41	−98.81	0.16*	−62.89*	1.06*	−4.46*
U1382B-9H4	15.88	−98.80	0.33*	−66.61*	1.04*	−4.47*
U1383D-2H3	14.73	−98.67	0.33*	−66.42*	1.69*	−4.44*
U1383D-4H2	14.67	−98.66	1.15	−65.61	0.66	−4.42
U1383D-5H4	12.23	−98.64	2.36	−66.57	1.02	−4.47

Note: NH_4^+ concentration was below the detection limit; therefore, the assumed concentration was 1 μM.

Denitrification: $5C_{27}H_{28}O_7 + 122NO_3^- + 4H_2O \rightarrow 13H^+ + 61N_2 + 135HCO_3^-$; Nitrification: $NH_4^+ + 2O_2 \rightarrow NO_3^- + H_2O + 2H^+$; N_2 fixation: $3C_{27}H_{28}O_7 + 222H_2O + 61N_2 + 41H^+ \rightarrow 122NH_4^+ + 81HCO_3^-$.

(LaRowe and Van Cappellen 2011), the amount of energy associated with the particular type of organic carbon in the sediments is closely captured by $C_{27}H_{28}O_7$.

Results

Site description and sediment geochemistry

Results from biostratigraphic analysis of the calcareous nanofossils indicate that the sediment within North Pond Hole U1383D ranged from Late Miocene to Pleistocene, the oldest age was determined to be approximately 5.6 Ma at the sediment-basement interface (Jang, Yi et al. 2014). Hole U1382B was not analyzed for sediment age; however, it is located only 5.9 km southwest of Hole U1383D, and the similarity of the sedimentary horizons at the two locations suggests comparable sediment ages (Expedition 336 Scientists 2012).

The oxygen concentration profile within the sediment column at North Pond has been previously discussed in a recent study (Orcutt et al. 2013). Hole U1382B was generally characterized by a zone of oxygenated sediment in the top 5 mbsf, followed by a depletion of oxygen concentrations in the mid-column to below detection limit (5 μM) with an oxic zone at the bottom of the sediment profile, about 70 mbsf, prior to the basement interface. North Pond Hole U1383D was characterized with an oxic zone within the first 9 mbsf, decreased to below detection limit at approximately 25 mbsf, then oxygen increased to 49 μM at approximately 42 mbsf. This has been described as a 'C' profile and was observed at all locations in North Pond (Orcutt et al. 2013).

The interstitial pore water that was collected from North Pond sediment shipboard has been published as a part of the IODP Expedition 336 Preliminary Report (Expedition 336 Scientists 2012); some of the data are represented in Figure 2. The average NO_3^- concentration was elevated compared to North Pond average bottom seawater (21.6 μM) (Ziebis et al. 2012), but was not significantly different between the two locations (33.2 μM in Hole U1382B and 29.1 μM in Hole U1383D). Concentrations of SO_4^{2-} and Cl^- remained unchanged downhole and were similar to seawater concentrations (Expedition 336 Scientists 2012). The concentration of NH_4^+ was below limit of detection (1.5 μM) in Hole U1382B; however, the concentration in Hole U1383D was 9.77 μM at 26 meters below seafloor (mbsf) and 7.08 μM at 36 mbsf. TOC and total nitrogen (TN) were analyzed onshore (Expedition 336 Scientists 2012) and were less than 0.2 and 0.1 weight % dry sediment, respectively (Figures 2b and e). The concentration of TOC was never more than 0.2% of the dry sediment weight and the TN did not exceed 0.1% of the dry sediment weight. Solid phase Fe and Mn did not exceed 3% by weight (Expedition 336 Scientists 2012).

Cell enumeration and 16S rRNA gene transcript abundance

Overall, the total cell abundance decreased with sediment depth, based on both epifluorescence microscopy cell counting and qPCR (Figure 3). At Hole U1382B, cell counts were highest ($5.8 \pm 0.09 \times 10^6$ cells/g) near the top section (2.9 mbsf), and lowest ($9.4 \pm 0.01 \times 10^5$ cells/g) near the basaltic basement (87.2 mbsf). The cell abundance in Hole U1383D was about an order of magnitude lower, but also decreased with depth from 2.2×10^5 cells/g in the surface sediment (1.0 mbsf) to 9.1×10^4 cells/g at the lowermost depth (47.7 mbsf). This trend of lower biomass at Hole U1383D compared to Hole U1382B is consistent with previous observations (Wankel et al. 2015).

The abundance of 16S rRNA gene transcripts within the sediment remained relatively consistent with depth (Figure 3). Within Hole U1382B, the abundance ranged from 5.1×10^4 transcripts g^{-1} at 7.3 mbsf to 2.8×10^4 transcripts g^{-1} at 84.3 mbsf. The transcript abundance in Hole U1383D was below the detection limit of the qPCR technique (10^3 transcripts g^{-1}) and could not be accurately quantified. Cell enumeration and transcript abundance data from this study are consistent with other published data for oligotrophic subsurface sediments (Kallmeyer et al. 2012; Mills et al. 2012).

Bacterial diversity

A total of 45,083 high-quality 16S rRNA gene sequences from the six DNA samples were generated from 454 pyrosequencing, covering the V1-V3 region, following removal of 8,895 sequences due to quality control and overlap with the negative extractions control and/or with drilling mud sequences. The average number of sequences per sample was 7,481, and the average read length was 477 bp after trimming. There was no significant difference in the number of OTUs in the DNA between Hole U1382B and U1383D, according to T-test results ($p > 0.05$). The percentage of unclassified sequences at the phylum level was less than 10%; however, at the genus level, 27% to 42% of the total sequences could not be classified.

A total of 29,751 16S rRNA gene transcripts passed quality control standards. A total of 10,222 sequences did not pass quality control and/or overlapped with extraction and drilling mud controls (Table 1), and were removed from the final set of sequences (Figure 6; Supplemental Figure 1). There were an average of 4,958 sequences per sample and an average read length of 467 base pairs after trimming. There was no statistically significant difference in the number of OTUs identified in each sample ($p = 0.076$), but the overall number of RNA OTUs was less than that of the DNA (Table 1). In general, the DNA sequences were significantly different from the RNA sequences (Figure 6). Less than 5% of the RNA sequences remained unclassified at the phylum level. At the genus level, 6% to 15% could not be classified. There was a notable difference between the percentage of sequences unclassified in the DNA and the RNA sequences, with the DNA having a greater number of unclassified sequences at the genus level (Figure 4). The calculated evenness and Shannon estimators were relatively consistent among the DNA sequences (e.g., more evenly distributed), but distribution was more variable among the RNA sequences (Table 1). Diversity decreased with depth in Hole 1383D and in Hole 1382B, the diversity was lowest at the mid-depth.

Overall, the greatest abundance of classified DNA sequences was most closely related to the phylum *Proteobacteria* (36–54% of all sequences), specifically *Alphaproteobacteria* (22–38%). Similarly, the greatest relative abundance of the 16S rRNA gene transcript (RNA) sequences were most closely related to the phylum *Proteobacteria* (−93%), with the classes

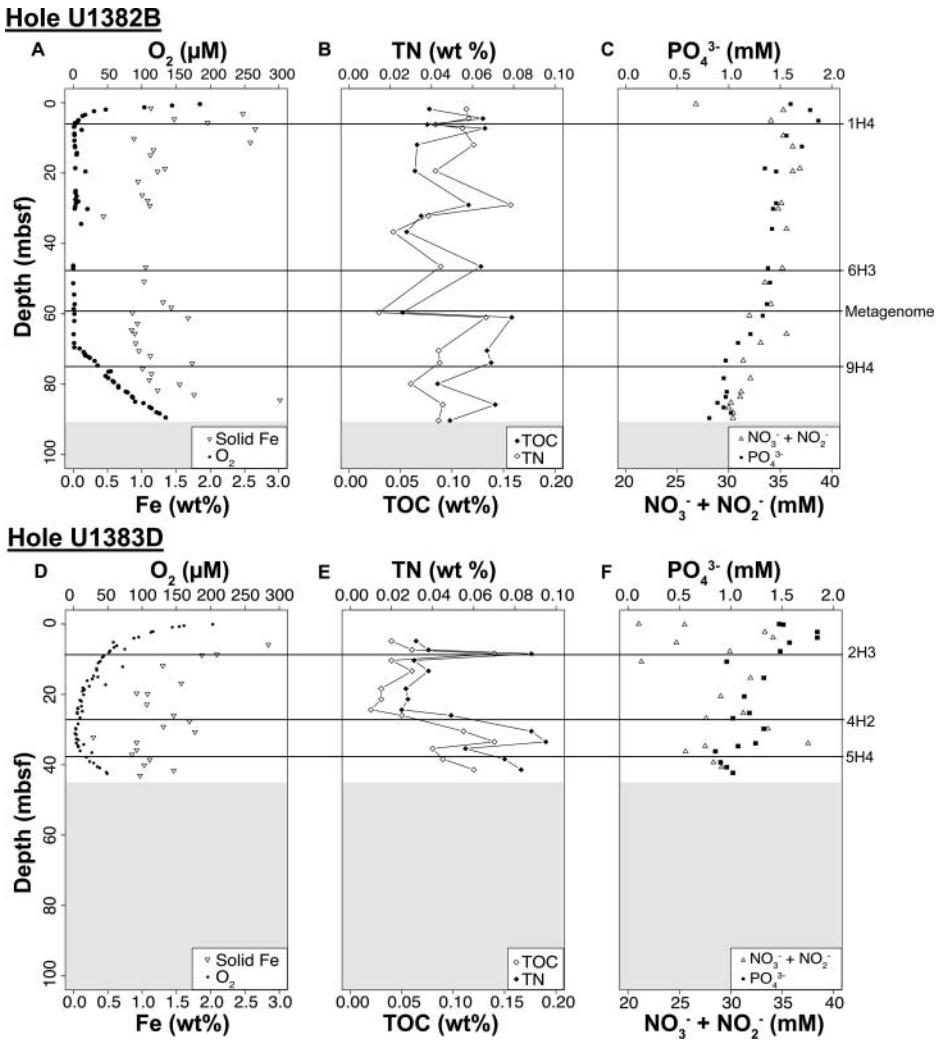

Figure 2. Sediment geochemical parameters with depth (in meters below seafloor, mbsf) in sediment from Holes U1382B (A-C) and U1383D (D-F), including dissolved oxygen and dissolved reduced iron (A and D), total nitrogen and organic carbon (B and E), and dissolved phosphate and nitrate (C and F). Grey shading indicates location of basement. Vertical lines denote the depth from which samples were collected. Oxygen data is reproduced here with permission from Orcutt et al. (2013). Iron, nitrate, and phosphate data from Expedition 336 (Expedition 336 Scientists, 2012).

Alphaproteobacteria (23–72%), *Betaproteobacteria* (11–26%), and *Gammaproteobacteria* (1–16%) representing the majority. The numerically dominant group within the active bacterial community was *Alphaproteobacteria*.

The next most abundant lineages in the DNA identified at the phylum level were *Cyanobacteria* (14–41%) and *Bacteroidetes* (5–15%; Figure 4). All of the samples contained sequences assigned to *Firmicutes* (1.3 −14.8%). No statistically significant trend was observed with depth or between the holes in the DNA sequences (Figure 6). Notable phyla within the RNA-based sequences included *Firmicutes* and *Bacteroidetes* (Figure 4). Sequences matching the *Firmicutes* phylum made up 3.7% to 14.1% of the total classified sequences.

The sequences that were most closely related to the *Cyanobacteria* phylum were further classified to the genus GpIIa. GpIIa were most abundant in the top of both Hole U1382B (29.9%) and Hole U1383D (16.7%). Chloroplast DNA, specifically from *Bacillariophyta* and *Chlorophyta* comprised 6.9% to 23.5% of the total classified DNA sequences. The most abundant were in the uppermost sample of Hole U1383D, near the surface. In contrast to the DNA sequences, the *Cyanobacteria* phylum comprised only 5.8% of the total classified RNA-derived reads that passed quality control in the shallowest sample of Hole U1382B (4.7 mbsf), 1.9% of the reads in the shallowest sample of Hole U1383D (8.9 mbsf), and 3.9% in the mid-depth of U1383D (26 mbsf). The *Cyanobacteria* sequences were classified as GpIIa and GpXIII. Chloroplast sequences were only detected in the RNA fraction in only one sample (U1382B-1H4).

Metagenomics

Metagenomic assembly of sequences from U1382B-7H5 resulted in 49,614 contigs with an average length of 461 bp. 55,598 putative protein coding sequences were queried for genes encoding proteins that mediate the nitrogen cycle. Putative coding sequences predicted to perform nitrate reduction/nitrate oxidation (*narG* and *narH*) were found in the metagenome (Figure 5). These sequences were most similar to *Alphaproteobacteria* and *Actinobacteria nar* genes. The nitrous oxide reducing indicator gene, *nosZ*, was identified. Genes related to DNRA genes (*nirB* and *nirD*) were also found in the metage-

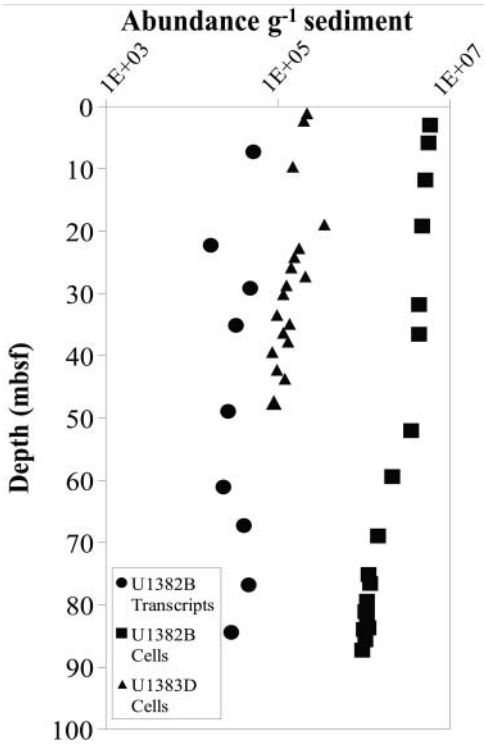

Figure 3. Transcript copies and cell density per gram of wet sediment from Holes U1382B and U1383D sediment. Standard deviations were too small to be depicted graphically.

nome. Like the *nar* genes, these were taxonomically assigned as *Alphaproteobacteria* and *Actinobacteria*. There was no evidence in the metagenome of genes involved in nitrite or nitric oxide reduction. Additionally, nitrogen fixation genes (NifDHK) similar to those from *Alphaproteobacteria* were found, but the taxonomic assignments were at a broad taxonomic level, so this assignment is not definitive.

Bioenergetics

As nitrogen-based metabolisms were expected to be important metabolisms supporting microbial communities throughout the sediment column, especially where oxygen was depleted (Wankel et al. 2015), we explored the thermodynamic energy yield for various oxidative and reductive nitrogen transformations based on sediment porewater chemical composition. The Gibbs free energies (ΔG_r) of denitrification, nitrification and nitrogen fixation in North Pond sediments at locations corresponding to the depths where nucleic acids were extracted are shown in Table 2, both in terms of energy yield per mole of electron transferred (kJ/(mol e-)) as well as in terms of energy yield per volume of sediment (J/cm^3), which takes into account concentrations, as described elsewhere (LaRowe et al. 2014; LaRowe and Amend 2015; Price et al. 2015; Teske et al. 2014). Based on both calculations, denitrification was the most favorable reaction of the three, yielding about 50% more Gibbs energy per mole of electron transferred versus nitrification, or ~5 to 13 times more energy than nitrification per cm^3 of sediment. Similarly, although nitrogen fixation was far less exergonic per mole of electron transferred, it provided virtually the same amount of energy as denitrification when viewed through the lens of limiting reactant. The estimated energy yield from denitrification and nitrogen fixation in the sediment column is consistent with nitrogen stable isotope evidence for these processes (Wankel et al. 2015).

Statistical analyses

Regression analyses were used to determine correlations between detected lineages and sediment composition for those identified as potential nitrate reducing bacteria (NRB; Figures 7a–c). We define this category of NRB as including sequences classified as: *Brevundimonas* (Tsubouchi et al. 2013), *Achromobacter* (Moore and Pickett 1960), *Mycobacterium* (Hartmans et al. 2006), *Methylophaga* (Doronina et al. 2003); *Corynebacterium* (Holt 1994), and *Staphylococcus* (Harms et al. 2003; Schleifer 2009). Although observed at all depths, the greatest abundance of active potential NRB was observed at Hole U1382B, particularly the oxic uppermost sample, and the lowest abundance was observed in the bottom depth of Hole U1383D (Figure 4). Additionally, the relative abundance of putative active nitrate reducing bacteria showed a strong inverse correlation ($R^2 = 0.82$) to total pore-water nitrogen (Figure 7a) and was most influenced by NO_3^- concentrations (Figure 7b). SVD analysis showed that the NRB percentage decreased with NO_3^- concentrations. Additionally, PCA also showed correlation between the putative NRB and NO_3^- (Figure 7b).

Discussion

Community structure

Statistically significant differences were noted between the DNA-based and RNA-based relative abundances of several phylogenetic groups within the North Pond sediment (Figure 4). The relative detection frequency of *Alphaproteobacteria*- and *Betaproteobacteria*-related sequences was significantly greater in RNA than in DNA ($p < 0.05$). However, the relative sequence abundance of *Cyanobacteria* and *Bacteroidetes* comprised a significantly greater abundance of DNA sequences than RNA ($p < 0.05$). Discrepancies between the RNA-based and DNA-based community structures may exist due to one lineage (e.g., OTU) being numerically abundant but having low metabolic activity (detected in the DNA analysis only), or being numerically limited but having high metabolic activity (detected in the RNA analysis only) (Mills et al. 2005; Moeseneder et al. 2005). The ratio of cell abundance to transcript abundance did not vary significantly with depth (Figure 3). The cell abundance, which is a measure of all cells, remained two orders of magnitude greater than the transcript abundance, which is a measure of active cells with detectable transcripts. We recognize that slight variations may occur between samples; therefore, the comparison between cell abundance and transcript abundance from samples located 10–20 cm apart should not be interpreted as strictly quantitative. While not a quantitative comparison, the trend that cell abundance was greater than RNA transcript abundance supports the conclusion that only a portion of the microbial community is active.

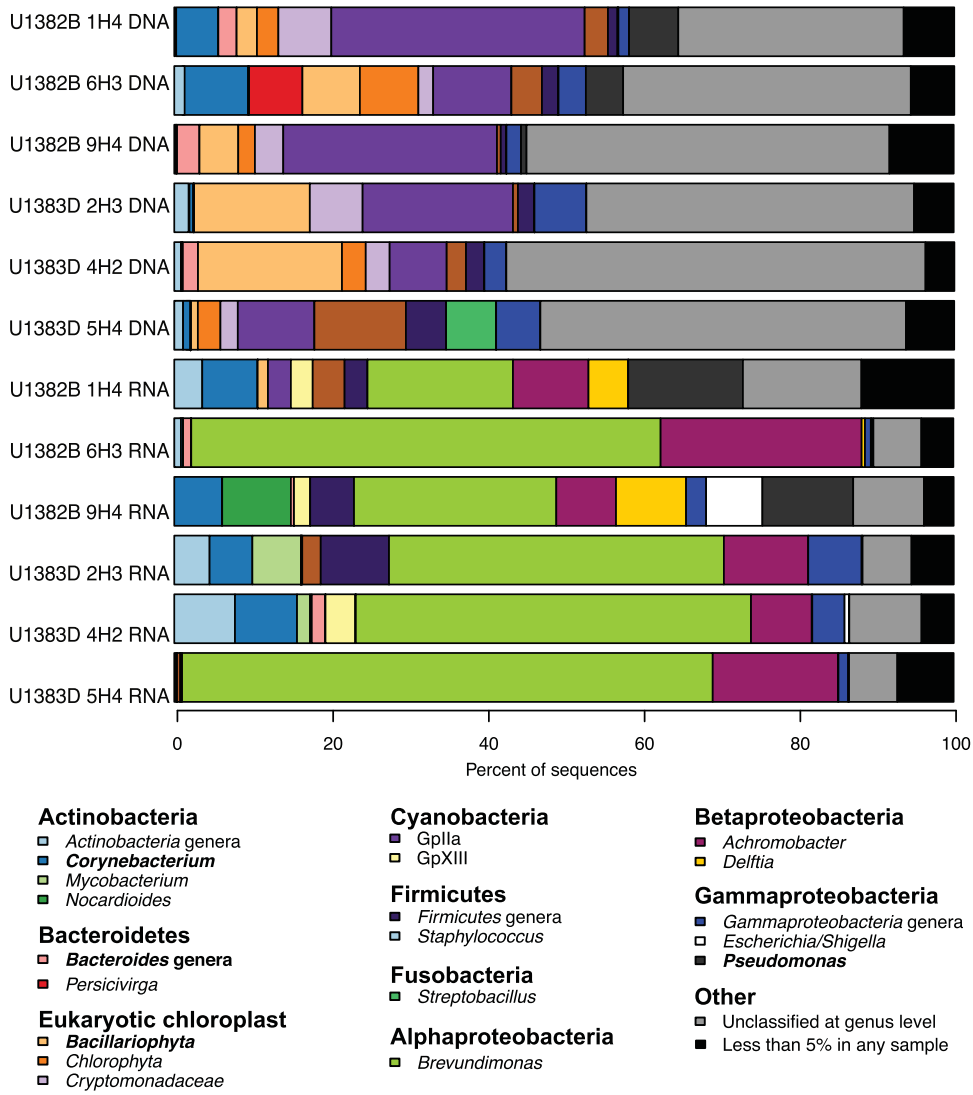

Figure 4. Relative percent abundance of genera present in greater than 1% in DNA- and RNA-derived 16S rRNA gene sequences from North Pond IODP Expedition 336 sediment samples. The genera in **bold** font are those that are putatively dormant.

Chloroplast preservation

A source of discrepancy between RNA-based and DNA-based microbial community structure analyses arises from the preservation of chloroplasts that are misclassified within taxonomic databases as *Cyanobacteria*. Sequences identified as *Cyanobacteria* averaged approximately 40% of the total DNA-derived sequences throughout all sediment depths, but were only identified in RNA sequences in the upper surface sediment (U1382B-1H4) at no more than 6% of the total sequences. Further investigation using Basic Local Alignment Search Tool (BLAST) against the NR database revealed that the *Cyanobacteria* sequences were mostly chloroplast DNA, classified as *Bacillariophyta* diatoms. A previous study of the upper meter of sediment from the same sample locations within North Pond from a predrilling survey expedition also detected *Bacillariophyta* in the sediment through rRNA transcript sequencing (Orsi et al. 2013b).

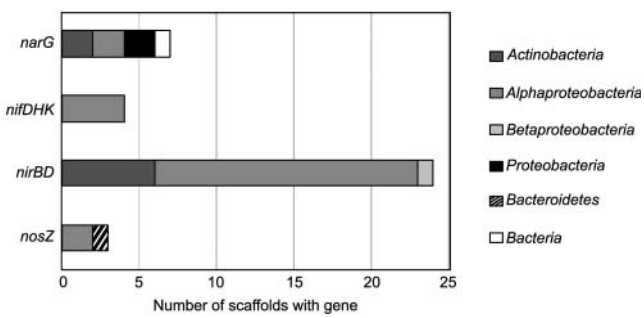

Figure 5. Bar chart of nitrogen cycling genes from the U1382B-7H5 metagenome.

Some *Bacillariophyta* genera have the potential to produce spores, or have the ability to enter into a dormant/inactive state (Jewson et al. 2008). It is likely that the chloroplast (containing 16S rRNA genes) of the *Bacillariophyta* was preserved in the cold, suboxic sediment of North Pond (Orsi et al. 2013a). This is not uncommon as the chloroplast of *Bacillariophyta* have been previously shown to be preferentially preserved in sediments dated to the middle Eocene (Wolfe et al. 2006), and

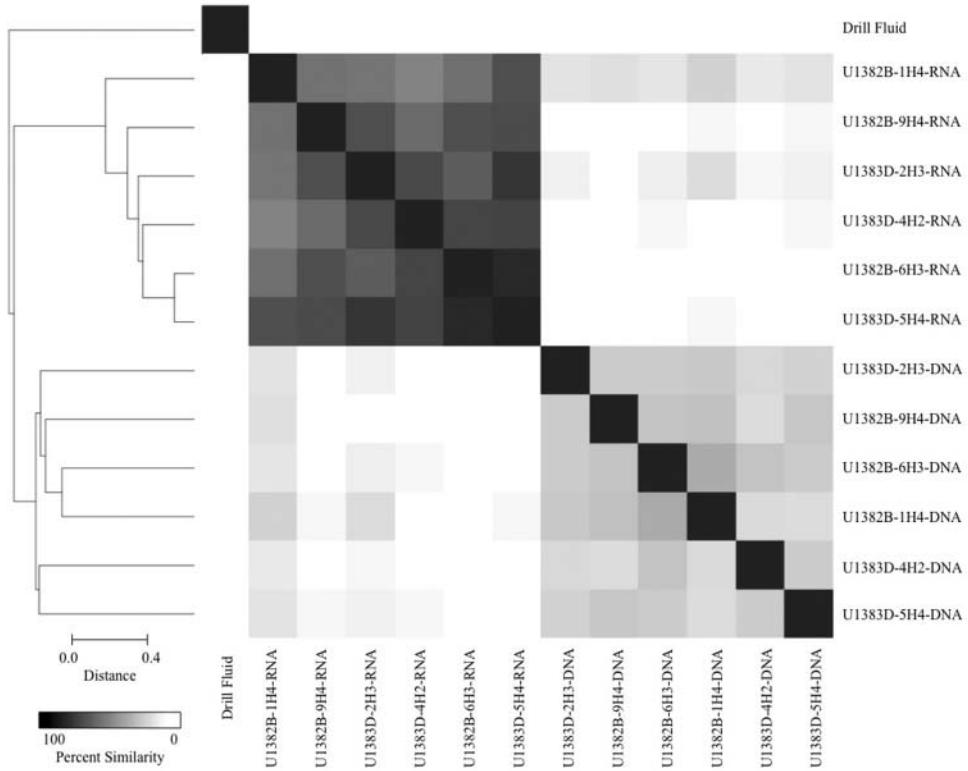

Figure 6. Dendrogram and heat map of the grouping of sequence libraries from each depth and site, including both DNA and RNA-derived 16S rRNA sequences. Sequences derived from the drilling fluid (Meyer et al. 2016) are included for comparison. Both the dendrogram and heat map show the clustering of sequences based on sequence type (i.e., DNA versus RNA-derived), and the higher similarity of the RNA-derived sequences between samples as compared to lower overlap in DNA-derived sequences between samples.

resting spores may be produced during low nutrient conditions (Kuwata and Takahashi 1990). Preservation of amplifiable rRNA genes from diatoms has been hypothesized to be possible due to low oxygen, low temperature conditions within sediments (Coolen et al. 2004), similar environment to that of North Pond. Chloroplast DNA from fossil diatoms was present throughout all sediment depths of the Bering Sea, ranging in age to 1.4 Ma (Kirkpatrick et al. 2016). This study showed that sequences identified as chloroplast declined with increasing sediment age, suggesting that a fraction of the chloroplast DNA is preserved.

Our current study determined that *Bacillariophyta* DNA was detected at depths of 77 mbsf. Additionally, we observed algal 16S rRNA gene-bearing chloroplast DNA from *Chlorphyta* and *Cryptomonadacea*, suggesting preservation of eukaryotic DNA in the 5 million-year-old subsurface sediment of North Pond. Our current dataset represents the first evidence for preservation of deeply buried (over 75 mbsf) eukaryotic chloroplast DNA.

Dormancy

Microbial dormancy is a physiological state of low metabolic activity, during which microbes do not grow and divide (Jones and Lennon 2010). Dormancy can be induced by many factors, including oxygen or resource stress (Kearns et al. 2016; Lewis 2007), as we expect to see in the oligotrophic sediments at North Pond. The Scout Model is one explanation of dormancy in which unfavorable environmental conditions cause microbial cells to enter an inactive state (Buerger et al. 2012; Epstein 2013). Dormant cells will stochastically activate, acting as a scout cell to determine if the environmental conditions are more favorable. If not, the scout cell dies; however, if the scout can survive it will form a new population (Epstein 2013), and potentially secrete chemical signals to 'wake up' the rest of the population, as seen in laboratory settings (Mukamolova et al. 2006; Wilmes et al. 2008).

Over 70% of the lineages in the North Pond DNA sequences have been described elsewhere as having the potential to be dormant or inactive, including *Bacillariophyta* (Jewson et al. 2008; Kuwata and Takahashi 1990), *Flavobacteriaceae* (Bakermans and Skidmore 2011), *Corynebacterium* (Seletzky et al. 2006), *Pseudomonas* (Kim et al. 2009), and *Leptospira* (Barragan et al. 2011). This is consistent with previous studies that have shown the proportion of inactive bacteria may be relatively low in eutrophic environments, but may account for up to 40% of taxon richness in oligotrophic systems (Jones and Lennon 2010; Novitsky 1987).

Overall, 16S rRNA gene abundance decreased with depth, though the transcript number stayed within the same order of magnitude (10^4 transcripts g^{-1}, Figure 3). Though rRNA content does not explicitly correlate with activity, rRNA content indicates the ability of an organism to produce protein and effect microbial activity (cf. Blazewicz et al., 2013). We examined the lineages capable of dormancy to detect if populations change their ability to produce proteins and potentially enter a dormant state between the top and middle of the sediment column (as oxygen and labile organics decrease), and reactivate in the lowest samples that have oxygen input from the basement. Some lineages simply decreased in rRNA sequence percent

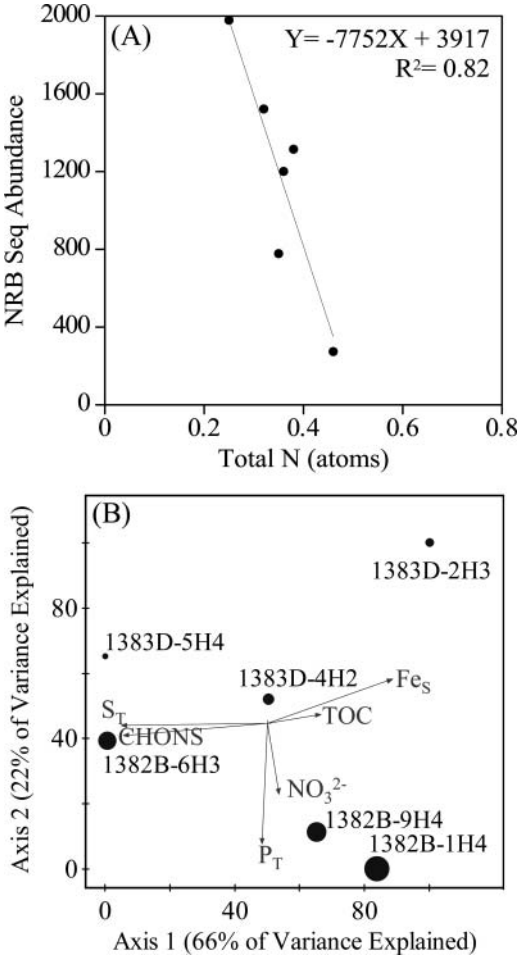

Figure 7. Regression (A) and principle component (B) analyses of RNA-derived sequence libraries with sediment geochemical parameters. (A) Regression analysis of abundance of sequences grouping within taxa presumed to be involved in nitrate reduction (i.e. nitrate reducing bacteria, NRB) versus nitrogen abundance in sediment reveals a negative correlation (i.e. higher NRB sequence abundance in low nitrogen sediment samples). (B) PCA analysis of NRB relative percent abundances within each site as they correspond to TOC, total sulfur atoms (S_T), nitrate (NO_3^{2-}), total phosphorus atoms (P_T), solid phase iron (Fe_S) and elemental carbon, hydrogen, oxygen, nitrogen and sulfur (CHONS). Dot size represents the relative abundance of NRB in each site. PCA also shows a correlation between the abundance of NRB and NO_3^{2-}.

with depth, and appear to never be dominant in rRNA samples. For instance, *Bacteroidetes* lineages decreased from the oxic top samples to the deepest, oxic samples, and the frequency of sequence detection for the *Bacteroidetes* phylum was statistically greater in the DNA analysis (~5–15%) compared to the RNA analysis (~1–3%) in the North Pond sediment. Other lineages showed support for the Scout model by showing higher percentages of the RNA derived community in the oxic samples (top and bottom) than in the middle samples (Figure 4). In both holes, *Bacilliales* decreased from top (7.1% in Hole U1382B and 10.9% in Hole U1383D) to middle (3.7% and 2.2%), then increased again in the oxic bottom sediment samples (6.3% and 4.9%). DNA sequences did not show the same pattern, with Hole U1382B exhibiting the highest percent of *Bacilliales* in the middle sample and Hole U1383D exhibiting the highest percent in the lowest sample, while the top and middle samples had very similar percentages (1.8% and 1.9%, respectively). Within the *Gammaproteobacteria, Pseudomonas* rRNA showed a similar pattern to the *Bacilliales* rRNA in Hole U1382B (14.9%:0.2%:10.7%), which was not mimicked by the DNA.

The metabolically active microbial community showed a statistically significant connection to the geochemical environment (Figure 7a–c); however, the total DNA-based population did not significantly correlate with any analyzed geochemical parameters. Similarly, regression analysis also showed no significant correlations between the total community and the geochemistry ($R^2 < 0.06$). This may be due to a majority of the total community being in a non-active state. This supports the concept that many microbes in subsurface settings such as North Pond are dormant. The increase of certain lineages from the middle, low-oxygen or anoxic samples to the deepest, oxic samples supports that in favorable conditions, inactive microbes can reactivate, lending support to the Scout model.

Nitrogen cycling metabolisms

The bioenergetics, metagenomic, 16S rRNA gene and transcript, and statistical analyses indicate that North Pond sediments contain active nitrogen cycling microbial community.

This finding is consistent with a recent study published quantifying nitrogen isotopic signatures in the North Pond deep subsurface (Wankel et al. 2015). In Wankel et al. (2015), the porewater nitrate isotopic composition in North Pond reflected active redox cycling of nitrogen, including the co-location of oxidative and reductive transformations. Thermodynamic calculations in the current study indicated that denitrification was the most energetically favorable reaction (Table 2). This supports the 16S rRNA gene data collected where the assignment of OTUs to bacteria genera with members capable of denitrification (1–15% of total sequences) and nitrate reduction (18–36% of total sequences) were the most numerically abundant sequences detected from the active fraction of the total population in the North Pond sediments (Figure 4). There is a negative correlation of sequences assigned as putatively NRB-related with pore-water nitrogen, suggesting that active denitrifiers could be responsible for the consumption of dissolved N. Active putative denitrifiers were most abundant in the top ~30 m and bottom ~70 m of site U1382B and in the top ~25 m of site U1383D. In the metagenome from sample U1382B-7H5, we see potential for dissimilatory nitrate reduction to ammonium and potential for nitrate reduction to nitrite. Again, this is consistent with Wankel et al. (2015) in which denitrification rates were greatest at the same depths where we found the greatest abundance of NRB. These results reflect findings in Osburn et al. (2014), which demonstrated that microbial community function followed geochemical predictions. This study extends those findings by examining functional gene capacities to further corroborate the putative functional assignments (Osburn et al. 2014).

The most frequently detected rRNA sequences within the active fraction of the microbial community were most closely related to the genus *Brevundimonas*, a marine bacterium that has been previously characterized as an aerobic heterotroph with the potential to reduce nitrate (Tsubouchi et al. 2013). Representative strains have been isolated from the western Mediterranean Sea (Fritz et al. 2005), deep subseafloor

sediment off the Shimokita Peninsula of Japan (Tsubouchi et al. 2013), and basaltic sand near Jeju Island, Korea (Choi et al. 2010). Although *Brevundimonas* was ubiquitous throughout all of the North Pond sediment samples here, a statistically significant negative correlation was observed between *Brevundimonas* sequence relative abundance and nitrate concentration according to regression analysis ($R^2 = 0.77$; $p<0.05$). Other notable genera that have been linked to nitrate reduction observed within the sequences from North Pond sediments included *Achromobacter* (Moore and Pickett 1960), *Mycobacterium* (Hartmans et al. 2006), *Corynebacterium* (Holt 1994), and *Methylophaga* (Doronina et al. 2003). *Achromobacter* was previously found in deep-sea sediments (18 mbsf) under the South Pacific Gyre, which is another region known to have limited productivity (D'Hondt et al. 2009; Zhang et al. 2014).

The contribution of ammonium to sediment nitrogen exchange depends heavily on the efficiency of nitrification. Nitrification was calculated to be an energetically favorable metabolism in the lower-most depths of Hole U1383D. Active potential nitrifying bacteria in North Pond included the genera *Micrococcus* (Stevens et al. 2002), *Bacillus* (Stevens et al. 2002), *Pseudomonas* (Stevens et al. 2002), *Staphylococcus* (Stevens et al. 2002), *Achromobacter* (Kundu et al. 2012; Quastel et al. 1952), and *Mycobacterium* (Kuenen and Robertson 1988). Within North Pond sediment, these active *Bacteria* with the potential for nitrification were co-located with nitrifying bacteria in zones of low oxygen and NH_4^+ accumulation (U1383D-4H2 and U1383D-5H4). Nitrate reduction and denitrification are often tightly coupled to nitrification in microaerophilic sediments (Jenkins and Kemp 1984; Seitzinger 1988), and the nitrate from nitrification can, in turn, be denitrified in a "cryptic" nitrogen cycle. The active, co-localization of these nitrifying and denitrifying bacteria would be an important factor on the balance of nitrification and denitrification within the North Pond sediment.

The reaction-diffusion model outlined in Wankel et al. (2015) provided evidence for extensive zones of overlap where O_2 and NO_3^- respiration (i.e., nitrification and denitrification) co-occur. Sequences related to known nitrifying genera were detected in all depths; however, the greatest frequency of NRB-related sequences was in the top and bottom depths of Hole U1382B and top of Hole U1383D. Supporting these results, Wankel et al. showed a similar trend of nitrification rates, the highest rates were calculated in the same depths that our greatest relative abundance of putative nitrifier-related sequences. Wankel et al. also found that nitrification rates were, at times, as much as an order of magnitude greater than the rates for denitrification, whereas our current study found that denitrification was the most energetically favorable metabolism (Table 2). Previous studies have shown that abiotic nitrification is possible in soil environments (Harper et al. 2015), which would result in higher nitrification rates. It is also possible that putative denitrifiers were more active than nitrifiers in North Pond, based on significantly greater detection frequency of 16S transcripts ($p < 0.05$), and the assumption that transcript abundance corresponds to activity. Additionally, some nitrifying bacteria are known to be able to switch to a denitrifying metabolism, and determining which is the active metabolism is difficult with through metagenomics and 16S rRNA-based analyses. It is also possible that all putative nitrifying bacteria have not been identified and Bacteria with unknown metabolisms are contributing to this pool. Future studies can build upon this data and determine the functional gene quantification to support the activity of the nitrifying and denitrifying metabolisms.

The capacity for N_2 fixation was also detected in the surface sediment at both locations, based on the presence of RNA sequences related to cultured bacterium that are capable of N_2 fixation. The bacterial genera with the capacity to fix N_2 included *Bradyrhizobium* (Jordan 1982; Kaneko et al. 2002), *Phyllobacterium* (Mantelin et al. 2006), *Devosia* (Romanenko et al. 2013), and *Stenotrophomonas* (Ryan et al. 2009). *Bradyrhizobium* and *Phyllobacterium* have also been previously co-located in Atlantis II Deep brine pool and Discovery Deep brine pool of the Red Sea (Wang et al. 2011).

The metagenome from U1382B-7H5 also included *nif* genes, which are associated with nitrogen fixation; however, nitrogen fixation would typically be considered energetically unfavorable in these sediments. This assumption is supported by the generally low frequency of detection for such lineages overall and the lack of quantifiable NH_4^+. The only measurable NH_4^+ accumulation was measured in the bottom two depths of Hole U1383D (25.9 and 38.7 mbsf). Wankel et al. determined that nitrogen fixation rates were so small that it was unlikely that this metabolism significantly impacts the nitrogen cycle at North Pond; they did calculate that nitrogen fixation was, in fact, occurring based on isotopic analysis. This is consistent with, and provides independent support for, the current study, in which we determined that active putative nitrogen fixers were present throughout all samples.

Our results suggest that several phylogenetic groups in North Pond oligotrophic sediment are inactive, with eukaryotic chloroplast DNA preserved in deeply buried sediment over 5 million years in age. The biogeochemical cycling of nitrogen was determined to be a critical active metabolism within North Pond, including the co-location of lineages related to organisms with the potential capacity for denitrification and nitrification, as well as, putative functional (DNA-based) evidence to suggest N_2 fixation. These findings are supported by recent geochemical evidence from North Pond (Wankel et al. 2015). The relative abundances of microorganisms detected in RNA sequences showed a significant correlation between putative function and geochemical concentrations, whereas DNA-based sequences did not. This suggests that future studies analyzing community structures in oligotrophic marine sediments should use RNA-based analysis to yield a more accurate representation of how microbial communities impact biogeochemical cycles within the deep subsurface.

Summary

The bacterial community within North Pond sediment was metabolically active and diverse. The total population (DNA-based analysis) contained more unique phylotypes that were more evenly distributed than the active fraction (RNA-based). Additionally, the DNA-based fraction had a considerable portion of the sequences related to eukaryotic chloroplasts resulting from diatom burial and potential preservation. These results skewed the relative abundances of the DNA-based bacterial community and suggested that a significant fraction of

the population may be inactive. The co-location of potential denitrifiers, nitrifiers, and N_2 fixers was observed. Of these groups, putative denitrifiers were the most frequently detected. Relative abundances of active lineages potentially capable of nitrate reduction were correlated with nitrate concentrations, whereas DNA-based analyses did not correlate with any of the reported geochemical parameters. This finding stresses the overall importance of determining both the active and total microbial populations when determining their influences on biogeochemical cycles.

Conflict of interest

The research was conducted in the absence of any commercial or financial relationships that could be construed as a potential conflict of interest.

Acknowledgments and funding

This research used samples and data provided by IODP. We thank the members of the crew and science party of IODP Expedition 336 for their assistance in sample collection. In particular, we thank Amanda Haddad, Hisako Hirayama, Steffen Leth Jørgensen, Heath Mills, and Joseph Russel for tireless efforts to collect samples on the ship, and C. Geoff Wheat and Samuel Hulme for porewater chemistry. We are also thankful for the helpful comments from Julie Koester and anonymous reviewers to improve the manuscript. This material is based upon work supported by the U.S. National Science Foundation under grants OCE-1344241 to PRG, OCE-1233226 to BNO, OCE-1233306 to KJE and the NSF-funded Science and Technology Center for Dark Energy Biosphere Investigations (C-DEBI; OCE-0939564 to KJE and JPA). This is C-DEBI contribution number 378. This work is dedicated to the memory of Katrina Edwards, a mentor, friend, and visionary in deep subsurface research.

References

Bakermans C, Skidmore ML. 2011. Microbial metabolism in ice and brine at −5 C. Environ Microbiol. 13(8):2269–2278.

Barragan VA, Mejia ME, Trávez A, Zapata S, Hartskeerl RA, Haake DA, Trueba GA. 2011. Interactions of *Leptospira* with environmental bacteria from surface water. Curr Microbiol. 62(6):1802–1806.

Biddle JF, Fitz-Gibbon S, Schuster SC, Brenchley JE, House CH. 2008. Metagenomic signatures of the Peru Margin subseafloor biosphere show a genetically distinct environment. Proc Nat Acad Sci. 105 (30):10583–10588.

Blazewicz SJ, Barnard RL, Daly RA, Firestone MK. 2013. Evaluating rRNA as an indicator of microbial activity in environmental communities: limitations and uses. ISME J. 7(11):2061. doi:10.1038/ismej.2013.102.

Bolger AM, Lohse M, Usadel B. 2014. Trimmomatic: a flexible trimmer for Illumina sequence data. Bioinformatics. 30(15):2114–2120.

Box GE, Cox DR. 1964. An analysis of transformations. J Royal Stat Soc Ser B (Methodological). 26(2):211–252.

Buerger S, Spoering A, Gavrish E, Leslin C, Ling L, Epstein S. 2012. Microbial scout hypothesis, stochastic exit from dormancy, and the nature of slow growers. Appl Environ Microbiol. 78(9):3221–3228.

Caporaso JG, Kuczynski J, Stombaugh J, Bittinger K, Bushman FD, Costello EK, Fierer N, Pena AG, Goodrich JK, Gordon JI. 2010. QIIME allows analysis of high-throughput community sequencing data. Nature Methods 7(5):335–336.

Choi J-H, Kim M-S, Roh SW, Bae J-W. 2010. *Brevundimonas basaltis* sp. nov., isolated from black sand. Int J Syst Evol Microbiol. 60(7):1488–1492.

Conner JK, Hartl DL. 2004. A primer of ecological genetics. Sinauer Associates Incorporated.

Coolen MJ, Muyzer G, Rijpstra WIC, Schouten S, Volkman JK, Damsté JSS. 2004. Combined DNA and lipid analyses of sediments reveal changes in Holocene haptophyte and diatom populations in an Antarctic lake. Earth Planet Sci Lett. 223(1):225–239.

Corinaldesi C, Barucca M, Luna G, Dell'Anno A. 2011. Preservation, origin and genetic imprint of extracellular DNA in permanently anoxic deep−sea sediments. Mol Ecol. 20(3):642–654.

DeSantis TZ, Hugenholtz P, Larsen N, Rojas M, Brodie EL, Keller K, Huber T, Dalevi D, Hu P, Andersen GL. 2006. Greengenes, a chimera-checked 16S rRNA gene database and workbench compatible with ARB. Appl and environ microbiology. 72(7):5069–5072.

D'Hondt S, Spivack AJ, Pockalny R, Ferdelman TG, Fischer JP, Kallmeyer J, Abrams LJ, Smith DC, Graham D, Hasiuk F, Schrum H, Stancin AM. 2009. Subseafloor sedimentary life in the South Pacific Gyre. Proc Nat Acad Sci. 106(28):11651–11656.

D'Hondt S, Inagaki F, Zarikian CA, Abrams LJ, Dubois N, Engelhardt T, Evans H, Ferdelman T, Gribsholt B, Harris RN. 2015. Presence of oxygen and aerobic communities from sea floor to basement in deep-sea sediments. Nat Geosci. 8(4):299–304.

Doronina NV, Darmaeva TD, Trotsenko YA. 2003. *Methylophaga alcalica* sp. nov., a novel alkaliphilic and moderately halophilic, obligately methylotrophic bacterium from an East Mongolian saline soda lake. Int J Syst Evol Microbiol. 53(1):223–229.

Dowd SE, Zaragoza J, Rodriguez JR, Oliver MJ, Payton PR. 2005. Windows. NET network distributed basic local alignment search toolkit (W.ND-BLAST). BMC Bioinformatics. 6:93.

Durbin AM, Teske A. 2011. Microbial diversity and stratification of South Pacific abyssal marine sediments. Environ Microbiol. 13(12):3219–3234.

Epstein S. 2013. The phenomenon of microbial uncultivability. Curr Opin Microbiol. 16(5):636–642.

Expedition 336 Scientists. 2012. Mid-Atlantic Ridge microbiology: Initiation of long-term coupled microbiological, geochemical, and hydrological experimentation within the seafloor at North Pond, western flank of the Mid-Atlantic Ridge. Integr Ocean Drilling Program: Preliminary Rep. 336:1–72.

Fritz I, Strömpl C, Nikitin DI, Lysenko A, Abraham W-R. 2005. Brevundimonas mediterranea sp. nov., a non-stalked species from the Mediterranean Sea. Int J Syst Evolutionary Microbiol. 55(1):479–486.

Giovannoni JJ, Wing RA, Ganal MW, Tanksley SD. 1991. Isolation of molecular markers from specific chromosomal intervals using DNA pools from existing mapping populations. Nucleic Acids Res. 19 (23):6553–6558.

Haas BJ, Gevers D, Earl AM, Feldgarden M, Ward DV, Giannoukos G, Ciulla D, Tabbaa D, Highlander SK, Sodergren E, Methe B, DeSantis TZ, Petrosino JF, Knight R, Birren BW, Human Microbiome C. 2011. Chimeric 16S rRNA sequence formation and detection in Sanger and 454-pyrosequenced PCR amplicons. Genome Res. 21(3):494–504.

Harms G, Layton AC, Dionisi HM, Gregory IR, Garrett VM, Hawkins SA, Robinson KG, Sayler GS. 2003. Real-time PCR quantification of nitrifying bacteria in a municipal wastewater treatment plant. Environ Sci Technol. 37(2):343–351.

Harper WF, Takeuchi Y, Riya S, Hosomi M, Terada A. 2015. Novel abiotic reactions increase nitrous oxide production during partial nitrification: Modeling and experiments. Chem Eng J. 281:1017–1023.

Hartmans S, de Bont JA, Stackebrandt E. 2006. The Genus Mycobacterium–Nonmedical. The Prokaryotes: Springer. pp. 889–918.

Helgeson HC. 1969. Thermodynamics of hydrothermal systems at elevated temperatures and pressures. Am J Sci. 267(7):729–804. doi:10.2475/ajs.267.7.729.

Helgeson HC, Kirkham DH, Flowers GC. 1981. Theoretical prediction of the thermodynamic behavior of aqueous electrolytes by high pressures and temperatures; IV, Calculation of activity coefficients, osmotic coefficients, and apparent molal and standard and relative partial molal properties to 600 degrees C and 5kb. American Journal of Science. 281 (10):1249–1516.

Holt JG. 1994. Bergey's Manual of Determinative Bacteriology. Baltimore: Williams & Wilkins.

Huse SM, Welch DBM, Voorhis A, Shipunova A, Morrison HG, Eren AM, Sogin ML. 2014. VAMPS: a website for visualization and analysis of microbial population structures. BMC Bioinformatics 15(1):1. doi:10.1186/1471-2105-15-41.

Huson DH, Auch AF, Qi J, Schuster SC. 2007. MEGAN analysis of metagenomic data. Genome Res. 17(3):377–386.

Hyatt D, Chen G-L, LoCascio PF, Land ML, Larimer FW, Hauser LJ. 2010. Prodigal: prokaryotic gene recognition and translation initiation site identification. BMC Bioinformatics 11(1):119. doi:10.1186/1471-2105-11-119.

Inagaki F, Hinrichs K-U, Kubo Y, Bowles M, Heuer V, Hong W-L, Hoshino T, Ijiri A, Imachi H, Ito M. 2015. Exploring deep microbial life in coal-bearing sediment down to ~ 2.5 km below the ocean floor. Sci. 349(6246):420–424.

Jang YS, Yi S, Park Y-S, Kim GY. 2014. Calcareous nannofossil biostratigraphy of North Pond area, Mid-Atlantic Ridge and its paleoenvironmental implication. Journal of the Geological Society of Korea. 50 (3):309–325.

Jenkins MC, Kemp WM. 1984. The coupling of nitrification and denitrification in two estuarine sediments. Limnol Oceanogr. 29(3):609–619.

Jewson DH, Granin NG, Zhdanov AA, Gorbunova LA, Bondarenko NA, Gnatovsky RY. 2008. Resting stages and ecology of the planktonic diatom *Aulacoseira skvortzowii* in Lake Baikal. Limnol Oceanogr. 53 (3):1125–1136.

Jin YO, Mattes TE. 2010. A Quantitative PCR Assay for Aerobic, Vinyl Chloride- and Ethene-Assimilating Microorganisms in Groundwater. Environ Sci & Tech. 44(23):9036–9041.

Jolliffe I. 2002. Principal component analysis and factor analysis. Springer Series in Statistics. New York: Wiley Online Library. pp. 50–166.

Jones SE, Lennon JT. 2010. Dormancy contributes to the maintenance of microbial diversity. Proc Nat Acad Sci USA. 107(13):5881–5886.

Jordan D. 1982. Transfer of Rhizobium japonicum Buchanan 1980 to *Bradyrhizobium* gen. nov., a genus of slow-growing, root nodule bacteria from leguminous plants. Int J Syst Bacteriol. 32(1):136–139.

Kallmeyer J, Pockalny R, Adhikari RR, Smith DC, D'Hondt S. 2012. Global distribution of microbial abundance and biomass in subseafloor sediment. Proc Nat Acad Sci USA. 109(40):16213–16216.

Kallmeyer J, Smith DC, Spivack AJ, D'Hondt S. 2008. New cell extraction procedure applied to deep subsurface sediments. Limnol Oceanogr: Methods 6(6):236–245.

Kanehisa M, Sato Y, Morishima K. 2016. BlastKOALA and GhostKOALA: KEGG tools for functional characterization of genome and metagenome sequences. J Mol Biol. 428(4):726–731.

Kaneko T, Nakamura Y, Sato S, Minamisawa K, Uchiumi T, Sasamoto S, Watanabe A, Idesawa K, Iriguchi M, Kawashima K. 2002. Complete genomic sequence of nitrogen-fixing symbiotic bacterium *Bradyrhizobium japonicum* USDA110. DNA Res. 9(6):189–197.

Kearns PJ, Angell JH, Howard EM, Deegan LA, Stanley RH, Bowen JL. 2016. Nutrient enrichment induces dormancy and decreases diversity of active bacteria in salt marsh sediments. Nat Commun. 7:12881. doi:10.1038/ncomms12881.

Kim J, Hahn J-S, Franklin MJ, Stewart PS, Yoon J. 2009. Tolerance of dormant and active cells in *Pseudomonas aeruginosa* PA01 biofilm to antimicrobial agents. J Antimicrob Chemother. 63(1):129–135.

Kirkpatrick JB, Walsh EA, D'Hondt S. 2016. Fossil DNA persistence and decay in marine sediment over hundred-thousand-year to million-year time scales. Geology 44(8):615–618.

Knights D, Kuczynski J, Charlson ES, Zaneveld J, Mozer MC, Collman RG, Bushman FD, Knight R, Kelley ST. 2011. Bayesian community-wide culture-independent microbial source tracking. Nature Methods 8 (9):761–763.

Kuenen JG, Robertson LA. 1988. Ecology of nitrification and denitrification. The Nitrogen and Sulphur Cycles. University of Southampton: 42nd Symposium of the Society for General Microbiology pp. 161–218.

Kundu P, Pramanik A, Mitra S, Choudhury JD, Mukherjee J, Mukherjee S. 2012. Heterotrophic nitrification by *Achromobacter xylosoxidans* S18 isolated from a small-scale slaughterhouse wastewater. Bioprocess Biosystems Eng. 35(5):721–728.

Kuwata A, Takahashi M. 1990. Life-form population responses of a marine planktonic diatom, *Chaetoceros pseudocurvisetus*, to oligotrophication in regionally upwelled water. Mar Biol. 107(3):503–512.

LaRowe D, Amend J, Kallmeyer J, Wagner D. 2014. Energetic constraints on life in marine deep sediments. Life in Extreme Environments: Microbial Life in the Deep Biosphere. Boston: De Gruyter. pp. 279–302.

LaRowe DE, Amend JP. 2015. Catabolic rates, population sizes and doubling/replacement times of microorganisms in natural settings. Am J Sci. 315(3):167–203.

LaRowe DE, Van Cappellen P. 2011. Degradation of natural organic matter: A thermodynamic analysis. Geochim Cosmochim Acta. 75 (8):2030–2042.

Lever MA, Alperin MJ, Teske A, Heuer VB, Schmidt F, Hinrichs KU, Morono Y, Masui N, Inagaki F. 2010. Acetogenesis in deep subseafloor sediments of the Juan de Fuca Ridge Flank: A synthesis of geochemical, thermodynamic, and gene-based evidence. Geomicrobiol J. 27(2):183–211.

Lever MA, Torti A, Eickenbusch P, Michaud AB, Šantl-Temkiv T, Jørgensen BB. 2015. A modular method for the extraction of DNA and RNA, and the separation of DNA pools from diverse environmental sample types. Front Microbiol. 6:476. doi:10.3389/fmicb.2015.00476.

Lewis K. 2007. Persister cells, dormancy and infectious disease. Nat Rev Microbiol. 5(1):48–56.

Lloyd KG, MacGregor BJ, Teske A. 2010. Quantitative PCR methods for RNA and DNA in marine sediments: Maximizing yield while overcoming inhibition. FEMS Microbiol Ecol. 72(1):143–151.

Lomstein BA, Langerhuus AT, D'Hondt S, Jørgensen BB, Spivack AJ. 2012. Endospore abundance, microbial growth and necromass turnover in deep sub-seafloor sediment. Nature 484(7392):101–104.

Mantelin S, Fischer-Le Saux M, Zakhia F, Béna G, Bonneau S, Jeder H, de Lajudie P, Cleyet-Marel J-C. 2006. Emended description of the genus Phyllobacterium and description of four novel species associated with plant roots: Phyllobacterium bourgognense sp. nov., Phyllobacterium ifriqiyense sp. nov., Phyllobacterium leguminum sp. nov. and Phyllobacterium brassicacearum sp. nov. Int J Syst Evol Microbiol. 56 (4):827–839.

Martin M. 2011. Cutadapt removes adapter sequences from high-throughput sequencing reads. EMBnet. J. 17(1):10–12.

McCune B, Mefford MJ. 1999. PC-ORD: Multivariate Analysis of Ecological Data. 6th ed.: MjM Software Design.

Meyer JL, Jaekel U, Tully BJ, Glazer BT, Wheat CG, Lin H-T, Hsieh C-C, Cowen JP, Hulme SM, Girguis PR. 2016. A distinct and active bacterial community in cold oxygenated fluids circulating beneath the western flank of the Mid-Atlantic ridge. Sci Rep. 6:22541. doi:10.1038/srep22541.

Mills HJ, Martinez RJ, Story S, Sobecky PA. 2005. Characterization of microbial community structure in Gulf of Mexico gas hydrates: Comparative analysis of DNA- and RNA-derived clone libraries. Appl Environ Microbiol. 71:3235–3247.

Mills HJ, Reese BK, St. Peter RC. 2012. Characterization of microbial population shifts during sample storage. Front Extreme Microbiol. (3):49.

Moeseneder MM, Arrieta JM, Herndl GJ. 2005. A comparison of DNA- and RNA-based clone libraries from the same marine bacterioplankton community. Fems Microbiol Ecol. 51(3):341–352.

Moore HB, Pickett M. 1960. The pseudomonas-achromobacter group. Can J Microbiol. 6(1):35–42.

Mukamolova GV, Murzin AG, Salina EG, Demina GR, Kell DB, Kaprelyants AS, Young M. 2006. Muralytic activity of Micrococcus luteus Rpf and its relationship to physiological activity in promoting bacterial growth and resuscitation. Mol Microbiol. 59(1):84–98.

Nadkarni MA, Martin FE, Jacques NA, Hunter N. 2002. Determination of bacterial load by real-time PCR using a broad-range (universal) probe and primer set. Microbiology-Sgm. 148:257–266.

Nogales B, Moore ERB, Abraham WR, Timmis KN. 1999. Identification of the metabolically active members of a bacterial community in a polychlorinated biphenyl-polluted moorland soil. Environ Microbiol. 1 (3):199–212.

Novitsky JA. 1987. Microbial growth rates and biomass production in a marine sediment: evidence for a very active but mostly nongrowing community. Appl Environ Microbiol. 53(10):2368–2372.

Orcutt BN, Wheat CG, Rouxel O, Hulme S, Edwards KJ, Bach W. 2013. Oxygen consumption rates in subseafloor basaltic crust derived from a reaction transport model. Nature Commun. 4.

Orsi W, Biddle JF, Edgcomb V. 2013a. Deep sequencing of subseafloor eukaryotic rRNA reveals active fungi across marine subsurface provinces. Plos One 8(2):e56335.

Orsi WD, Edgcomb VP, Christman GD, Biddle JF. 2013b. Gene expression in the deep biosphere. Nature 499(7457):205–208.

Osburn MR, LaRowe DE, Momper LM, Amend JP. 2014. Chemolithotrophy in the continental deep subsurface: Sanford Underground Research Facility (SURF), USA. Front Microbiol. 5: 610.

Peng Y, Leung HC, Yiu S-M, Chin FY. 2012. IDBA-UD: a de novo assembler for single-cell and metagenomic sequencing data with highly uneven depth. Bioinformatics 28(11):1420–1428. doi:10.1093/bioinformatics/bts174.

Price RE, LaRowe DE, Italiano F, Savov I, Pichler T, Amend JP. 2015. Subsurface hydrothermal processes and the bioenergetics of chemolithoautotrophy at the shallow-sea vents off Panarea Island (Italy). Chem Geol. 407:21–45.

Quastel J, Scholefield P, Stevenson J. 1952. Oxidation of pyruvic acid oxime by soil organisms. Biochem. J. 51(2):278. doi:10.1042/bj0510278.

Reese BK, Mills HJ, Dowd SE, Morse JW. 2013. Linking molecular microbial ecology to geochemistry in a coastal hypoxic zone. Geomicrobiol J. 30(2):160–172.

Romanenko LA, Tanaka N, Svetashev VI. 2013. *Devosia submarina* sp. nov., isolated from deep-sea surface sediments. Int J Syst Evol Microbiol. 63(Pt 8):3079–3085.

Ryan RP, Monchy S, Cardinale M, Taghavi S, Crossman L, Avison MB, Berg G, van der Lelie D, Dow JM. 2009. The versatility and adaptation of bacteria from the genus *Stenotrophomonas*. Nat Rev Microbiol. 7 (7):514–525.

Schleifer K-H. 2009. Phylum XIII. Firmicutes In: Gibbons, Murray, editors. Bergey's Manual of Systematic Bacteriology. Springer. pp. 1317–1319.

Schloss PD, Westcott SL, Ryabin T, Hall JR, Hartmann M, Hollister EB, Lesniewski RA, Oakley BB, Parks DH, Robinson CJ, Sahl JW, Stres B, Thallinger GG, Van Horn DJ, Weber CF. 2009. Introducing mothur: Open-source, platform-independent, community-supported software for describing and comparing microbial communities. Appl Environ Microbiol. 75(23):7537–7541.

Schulte MD, Shock EL, Wood RH. 2001. The temperature dependence of the standard-state thermodynamic properties of aqueous nonelectrolytes. Geochim Cosmochim Acta. 65(21):3919–3930.

Seitzinger SP. 1988. Denitrification in freshwater and coastal marine ecosystems: ecological and geochemical significance. Limnol Oceanogr. 33:702–724.

Seletzky JM, Noack U, Fricke J, Hahn S, Büchs J. 2006. Metabolic activity of *Corynebacterium glutamicum* grown on L-lactic acid under stress. Appl. Microbiol Biotechnol. 72(6):1297–1307.

Shock EL, Helgeson HC. 1988. Calculation of the thermodynamic and transport properties of aqueous species at high pressures and temperatures: Correlation algorithms for ionic species and equation of state predictions to 5 kb and 1000 C. Geochim Cosmochim Acta. 52 (8):2009–2036.

Shock EL, Helgeson HC. 1990. Calculation of the thermodynamic and transport properties of aqueous species at high pressures and temperatures: Standard partial molal properties of organic species. Geochim Cosmochim Acta. 54(4):915–945.

Shock EL, Helgeson HC, Sverjensky DA. 1989. Calculation of the thermodynamic and transport properties of aqueous species at high pressures and temperatures: Standard partial molal properties of inorganic neutral species. Geochim Cosmochim Acta. 53(9):2157–2183.

Shock EL, Oelkers EH, Johnson JW, Sverjensky DA, Helgeson HC. 1992. Calculation of the thermodynamic properties of aqueous species at high pressures and temperatures. Effective electrostatic radii, dissociation constants and standard partial molal properties to 1000 C and 5 kbar. Journal of the Chemical Society, Faraday Transactions. 88 (6):803–826.

Stein R, Blackman D, Inagaki F, Larsen H-C. 2014. Earth and Life Processes Discovered from Subseafloor Environments: A Decade of Science Achieved by the Integrated Ocean Drilling Program (IODP). Amsterdam: Elsevier.

Stevens W, Drysdale G, Bux F. 2002. Evaluation of nitrification by heterotrophic bacteria in biological nutrient removal processes: Research in action. S Afr J Sci. 98(5-6):222–224.

Tanger JC, Helgeson HC. 1988. Calculation of the thermodynamic and transport properties of aqueous species at high pressures and temperatures; revised equations of state for the standard partial molal properties of ions and electrolytes. American Journal of Science. 288(1):19–98.

Teske A, Callaghan AV, LaRowe DE. 2014. Biosphere frontiers of subsurface life in the sedimented hydrothermal system of Guaymas Basin. Front Microbiol. 5:362. doi:10.3389/fmicb.2014.00362.

Torti A, Lever MA, Jørgensen BB. 2015. Origin, dynamics, and implications of extracellular DNA pools in marine sediments. Mar Genomics 24:185–196.

Tsubouchi T, Shimane Y, Usui K, Shimamura S, Mori K, Hiraki T, Tame A, Uematsu K, Maruyama T, Hatada Y. 2013. *Brevundimonas abyssalis* sp. nov., a dimorphic prosthecate bacterium isolated from deep-subsea floor sediment. Int J Syst Evol Microbiol. 63(6):1987–1994.

Vineis JH, Ringus DL, Morrison HG, Delmont TO, Dalal S, Raffals LH, Antonopoulos DA, Rubin DT, Eren AM, Chang EB. 2016. Patient-Specific Bacteroides Genome Variants in Pouchitis. mBio. 7 (6):e01713–16.

Wang Q, Garrity GM, Tiedje JM, Cole JR. 2007. Naive Bayesian classifier for rapid assignment of rRNA sequences into the new bacterial taxonomy. Appl and Environ Microbiology. 73(16):5261–5267.

Wang Y, Yang J, Lee OO, Dash S, Lau SC, Al-Suwailem A, Wong TY, Danchin A, Qian P-Y. 2011. Hydrothermally generated aromatic compounds are consumed by bacteria colonizing in Atlantis II Deep of the Red Sea. ISME J. 5(10):1652–1659.

Wankel SD, Buchwald C, Ziebis W, Wenk CB, Lehmann MF. 2015. Nitrogen cycling in the subsurface biosphere: nitrate isotopes in porewaters underlying the oligotrophic North Atlantic. Biogeosci Discuss. 12 (16):13545–13591.

Wilmes P, Andersson AF, Lefsrud MG, Wexler M, Shah M, Zhang B, Hettich RL, Bond PL, VerBerkmoes NC, Banfield JF. 2008. Community proteogenomics highlights microbial strain-variant protein expression within activated sludge performing enhanced biological phosphorus removal. ISME J. 2(8):853–864.

Wolfe AP, Edlund MB, Sweet AR, Creighton SD. 2006. A first account of organelle preservation in Eocene nonmarine diatoms: Observations and paleobiological implications. Palaios 21(3):298–304.

Zhang Z, Fan X, Gao X, Zhang X-H. 2014. Achromobacter sediminum sp. nov., isolated from deep subseafloor sediment of South Pacific Gyre. Int J Syst Evolutionary Microbiol. 64(7):2244–2249.

Ziebis W, McManus J, Ferdelman T, Schmidt-Schierhorn F, Bach W, Muratli J, Edwards KJ, Villinger H. 2012. Interstitial fluid chemistry of sediments underlying the North Atlantic gyre and the influence of subsurface fluid flow. Earth Planet Sci Lett. 323:79–91.